# Observation of Atomic Place Exchange in Submonolayer Heteroepitaxial Fe/Au(001) Films

Y.-L. He and G.-C. Wang

*Physics Department, Rensselaer Polytechnic Institute, Troy, New York 12180-3590*

(Received 10 March 1993)

Submonolayer Fe films on a Au(001) surface were found to exhibit atomic place exchanges with Au atoms during room temperature growth by using the angular profile measurement of high-resolution low-energy electron diffraction. The place exchanged atoms result in 2D Au surface islands and Fe subsurface structures. These inverted 2D islands form a structure with a roughly equal island size and spacing in ~0.5 monolayer Fe/Au(001) surfaces. The observed mechanism of the atomic place exchange is consistent with recent first-principles calculations for a heteroepitaxial system.

PACS numbers: 68.55.Jk, 61.14.Hg, 68.35.Bs, 68.35.Fx

Epitaxial growth and interface diffusion of metal films on metal substrates have been subjects of both theoretical and experimental studies recently. Theoretical modelings, such as molecular dynamics simulations based on realistic atomic potentials and first-principles total energy calculations, have indicated that atomic place exchange may be an important mechanism in surface interdiffusion and surface self-diffusion [1]. Experimental results consistent with the atomic place exchange have been obtained by field ion microscopy [2], x-ray photoelectron and Auger electron forward scattering [3–5], low energy ion scattering [6], and scanning tunneling microscopy [7] techniques. For a metal on metal system, it has been explained that the atomic place exchange results in the formation of a subsurface structure during initial growth [8]. This growth mechanism is quite different from the three well-known conventional growth modes [9]. In this Letter, we report the observation of subsurface inversion through atomic place exchange in the initial growth of Fe on Au(001), using the constructive and destructive interference of low-energy electron waves. This diffraction technique allows us to determine not only the degree of atomic place exchange but also for the first time the distribution of exchanged atoms in submonolayer films.

The submonolayer Fe films were deposited on a Au(001) surface at ~310 K in a UHV chamber equipped with high-resolution low-energy electron diffraction (HRLEED) [10] and Auger electron spectroscopy. The Fe molecular beam epitaxy source consists of an Fe foil with 99.99% purity and 0.5 mm thickness. The deposition rate has been determined by analyses of the shape changes of angular profiles of the (00) beam measured from the Fe/Au(001) surface (to be discussed later). Typically, the growth rate is ~0.55 ML/min (ML denotes monolayer) with the Fe source held at ~1200 K. The terrace size in the reconstructed Au(001) surface ranges from ~400 to ~600 Å. The (001) surface unit meshes for both fcc Au and bcc Fe are square (2.88×2.88 Å and 2.87×2.87 Å, respectively), differing by only ~0.4%. After a submonolayer Fe film was prepared, a (1×1) LEED pattern was observed. The angular profile of the (00) beam was measured either as a function of primary electron energy at a fixed temperature to characterize the interface morphology, which includes islands distribution and types of steps, or as a function of temperature.

The physical principle of the angular profile of a diffraction beam in LEED has been reviewed extensively [11]. The angular profile may have various shapes, depending on the morphology of the surface and the diffraction condition. If there are atomic steps on the surface, the path lengths of electron waves scattered from adjacent terraces will be different upon reaching the detector. When the path length difference $D_{PL}$ equals an integral number of the electron wavelength, the angular profile remains the same as the instrument response function as if there was no step on the surface. This is the constructive interference condition or the in-phase diffraction condition, $D_{PL}=2d\cos\theta=n\lambda$, where $d$ is the step height, $\theta$ is the angles of incidence and diffraction for the (00) beam, $n$ is the order of diffraction, and the electron wavelength $\lambda=[150.4/E(\text{eV})]^{1/2}$. In contrast, if the path difference equals half an integral number of the electron wavelength, the destructive interference occurs and the angular profile will be the broadest. This is the out-of-phase diffraction condition, $2d\cos\theta=(n+\frac{1}{2})\lambda$. For a surface with random up and down steps, the full width at half maximum at the out-of-phase condition is inversely proportional to the average terrace size. Based on this simple interference concept, one can derive $E_n(\text{eV})=150.4n^2/(2d\cos\theta)^2$. Table I lists both the calculated and measured energies corresponding to various diffraction conditions for surfaces with a Au-Au step, an Fe-Fe step, and an Fe-Au step. The measured energies for pure Au(001) and Fe(001) surfaces agree well with

TABLE I. Diffraction conditions of the (00) beam. The bulk interlayer spacings are used in the calculations and the diffraction angle is 3.75°.

| Method | System | $d$ (Å) | $E_{3/2}$ (eV) | $E_2$ (eV) |
|---|---|---|---|---|
| Calculation | Au-Au | 2.04 | 20.4 | 36.3 |
| | Fe-Fe | 1.44 | 41.0 | 72.8 |
| | Averaged | | | |
| | Fe-Au | 1.74 | 28.1 | 49.9 |
| Experiment | Au-Au | 2.04 ± 0.01 | 20.4 ± 0.3 | 36.3 ± 0.5 |
| | Fe-Fe | 1.44 ± 0.02 | 41.0 ± 1.0 | 72.8 ± 1.8 |
| | Fe-Au | 1.82 ± 0.01 | 25.6 ± 0.4 | 45.6 ± 0.7 |



0031-9007/93/71(23)/3834(4)$06.00

the calculations. As one can see from the table, for the same order of out-of-phase diffraction, e.g., $n=\frac{3}{2}$, the energy varies from 20.4 to 41.0 eV when the step height changes from 2.04 to 1.44 Å. From the measured destructive condition, 25.5 eV, one can calculate the step height for Fe/Au(001) submonolayers to be $\sim$1.82 Å. One may use this sensitive energy change of the out-of-phase condition to identify the type of steps present in a heteroepitaxial interface, and even to study 2D versus 3D growth modes [12].

Figure 1 shows the angular profiles at 25.5 eV during deposition of Fe on Au(001). The angular profile changes drastically with accumulated Fe deposition time. At 110 sec, the angular profile becomes nearly the same as the initial time. This means the ordering of the Fe/Au(001) surface is virtually identical to that of the clean Au(001) surface. Therefore, we assign the Fe coverage to be $\sim$1 ML at $t=110$ sec. Note that at a deposition time of $\sim$55 sec the angular profile shows a central peak with additional satellite side peaks that actually form a ring in a 2D intensity map (not shown here). Similar angular profiles have been observed on W/W(001), Cu/Cu(100), Fe/Ag(001), and Ag/Ge(111) [13]. The triple peak profile is consistent with a profile obtained from a two level stepped surface with a roughly equal island size and spacing (the distance between adjacent island edges) near an out-of-phase condition [14]. We judge that the Fe coverage at 55 sec is very close to $\sim$0.5 ML. Shifting the energy even $\sim$1 eV away from 25.5 eV significantly increases the central peak intensity,

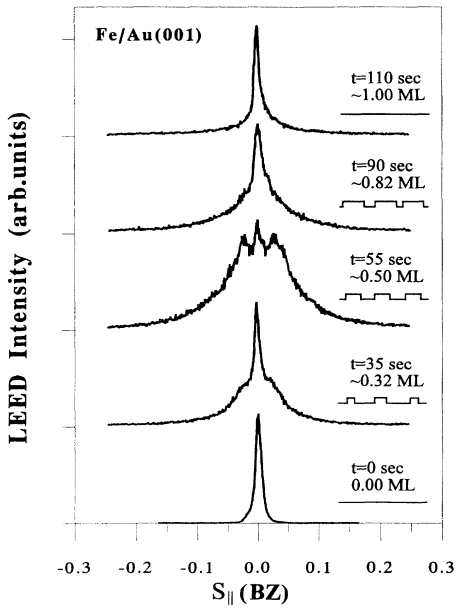


FIG. 1. Angular profiles of the (00) beam measured along the [110] direction and at the out-of-phase condition, 25.5 eV, during submonolayer growth. The profiles are symmetric in all azimuthal directions. The insets are sketches of the 2D island distributions. The Brillouin zone (BZ) equals $\sim$2.18 Å$^{-1}$ for both bcc Fe(001) and fcc Au(001) surfaces.

while decreasing the satellite peak intensity. This sensitive energy dependence implies $E\approx 25.5$ eV corresponds to an out-of-phase diffraction condition, $n=\frac{3}{2}$, with a step height of 1.82 Å; see Table I. Very narrow angular profiles similar to the instrument response function are also observed in the neighborhood of 45.5 eV during the entire submonolayer growth, which suggests an in-phase diffraction condition, $n=2$. With the consistency of these diffraction conditions, we realize that the actual Fe-Au step height in the submonolayer films may simply be the average of bulk interlayer lattice spacings with a few percent expansion, 1.82 vs 1.74 Å. The energy dependent angular profiles do not show any broadening near the Fe-Fe out-of-phase condition, 41 eV, indicating no 3D formation of Fe islands [12]. Both the profiles measured at $\sim$0.32 and $\sim$0.82 ML consist of a central peak and a diffuse shoulder. For $\sim$0.5 ML films, the observed ring structure implies a two level system [14], where both the island size and the spacing are about the same size. The shouldered structure observed away from $\sim$0.5 ML is consistent with a two level system with both island size and spacing following different preferred sizes.

The structure of $\sim$0.5 ML film can be further quantified by decomposing the measured angular profiles. The results are shown as dotted curves in Fig. 2. The angular profile can be best fitted by two 1D Lorentzians and one Gaussian. The inverse of half the separation of the two Lorentzian peaks, the ring radius $\sim$0.049 Å$^{-1}$, yields an island size and spacing of $\sim$130 Å. The individual Lorentzian represents the deviations of island sizes and spacings from the preferred value. The Lorentzian width (ring width), $\sim$0.133 Å$^{-1}$, indicates a real space deviation of $\sim$50 Å. The ring radius and width give us a Au island dimension of $\sim 130\pm 50$ Å, which is smaller than the terrace width. The Gaussian, resulted from the coherent scattering of electrons from the surface, is the

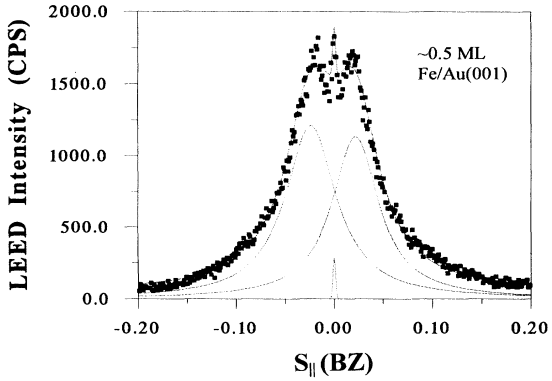


FIG. 2. A (00) beam angular profile measured at the out-of-phase condition and $\sim$0.5 ML Fe coverage. The 3D diffraction profile consists of a ringlike structure centered around the Bragg rod. The two dotted curves away from the Bragg peak represent two 1D Lorentzians. The Gaussian component is centered at the Bragg spot. The dotted curve through the data points is the sum of those three components. CPS stands for counts per second.

instrument response function.

Figure 3 shows normalized angular profiles of the (00) beam measured at the in-phase condition, 45.5 eV, for various temperatures. Surprisingly, these profiles are essentially independent of temperature. If inhomogeneity was present on the surface at elevated temperatures, a line shape with a sharp central spike sitting on a diffuse shoulder would be expected at the in-phase condition [15]. The inhomogeneity here describes lateral local variation of the scattering amplitude. If a stepless surface with patches of Au and Fe smoothly adjoining each other would produce wings on the Bragg rod. The lateral local variations of the scattering amplitude between the Fe and Au patches change the in-phase condition for a homogeneous surface to a non-in-phase condition. Thus, the diffuse shoulder would appear at the in-phase condition. This contradicts the experimental findings and leads us to the conclusion that the islands are Au. The long-range ordering of the surface contributes to the sharp central spike. The spike-on-shoulder line shape has been observed for the inhomogeneous mixing of Ni/Si, $SiO_2$/Si [16], and thicker layer Fe/Au(001) [17] at in-phase conditions.

We fitted the angular profile at the in-phase condition with two components, an instrument response function representing the long-range coherent scattering and a Lorentzian representing the scattering from possible local inhomogeneity regions. The best fit to the angular profile, shown as the solid curve in Fig. 3, consists of only the instrument response. That the diffuse shouldered profile underneath the central spike was not observed in Fig. 3 is an indication that the electrons see a homogeneous surface. One can exclude other possibilities such as Fe islands on top of Au substrate, since this corresponds to an inhomogeneous surface and thus the diffuse shouldered profile would show up in Fig. 3. Another possible case is

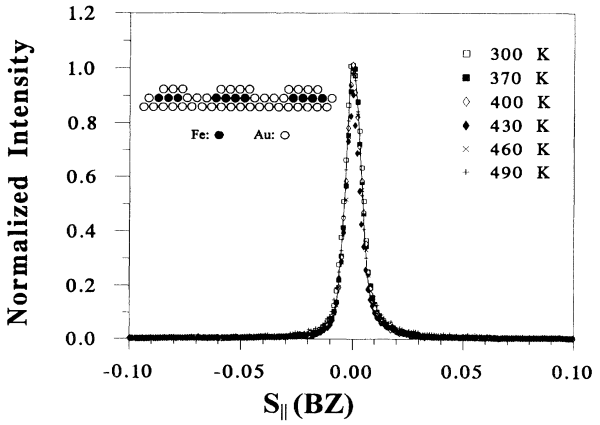


FIG. 3. The (00) beam angular profiles measured at the in-phase condition, 45.5 eV, and ~0.5 ML Fe coverage for various annealing temperatures. The normalized angular profiles are superimposed well. The inset is a sketch of the interface morphology. Note that the Fe submonolayer is inverted into the second layer through atomic place exchanges.

the ordered surface alloy which would contribute to superlattice beams, in contrast to the $(1\times1)$ pattern as we observed. This important result confirms that the Fe atoms already exchanged their places with Au atoms during deposition at room temperature. Hence, the diffraction would not be able to show any Fe-Au inhomogeneity on the surface since the top surface consists of only Au atoms at room temperature and beyond. We propose the interface morphology for ~0.5 ML film, shown as an inset in Fig. 3. The submonolayer Fe film made an inversion into the second layer from the surface. The Au surface islands are coupled on top of the Fe subsurface islands in the Fe/Au(001) interface. At this coverage, both the surface Au and subsurface Fe islands form a structure with roughly equal island size and spacing.

To achieve the proposed interface structure, the settlement of a freshly deposited Fe adatom may involve surface diffusion to an adlayer island, then a vertical atomic place exchange with a surface Au atom. This structure is consistent with a scanning tunneling microscopy study of Au/Ag(110) [7] and first-principles calculations for 1 ML Au on Ag(110), where an inverted interface with the Au monolayer covered by 1 ML Ag is the most energetically favorable [8]. The uniformity of the 2D island size implies that the Fe adatom prefers to attach to smaller islands. An alternative process leading to the Au surface structure is that the freshly deposited Fe atom first makes a place exchange with a surface Au atom. The resulted Au adatom then attaches to an island through surface diffusion. However, this random atomic place exchange results in a random Fe subsurface. Random Fe subsurface population would also lead to inhomogeneity (islands of Au on a sea of mixed Fe/Au) which conflicts with the findings at the in-phase condition.

We may further study the interface structure at the out-of-phase condition. Figure 4 shows angular profiles of the (00) beam measured at the out-of-phase condition for various temperatures. The profiles basically retain the same shape up to ~385 K. The ring structure deteriorates drastically at ~460 K due to partial loss of Fe into the bulk. Beyond ~490 K, diffuse $\frac{1}{5}$ beams of clean Au(001) reconstruction reappear, implying further Fe diffusion into the bulk. At ~515 K, the ring structure completely diminishes and the $\frac{1}{5}$ beams are clearly observed. If the inhomogeneity was introduced onto the surface by Fe and Au intermixing at elevated temperatures, there would be one more Lorentzian component added to the room temperature angular profile as discussed for the in-phase condition. However, the best fit to the angular profile does not require such a component over the entire temperature range. The absence of the Lorentzian is consistent with that from the angular profiles at the in-phase condition. With the method applied in Fig. 2, we have fitted all the temperature dependent profiles including those in Fig. 4. The results show both ring radius and individual Lorentzian width remain nearly constant below ~385 K. Drastic drops of the ra-

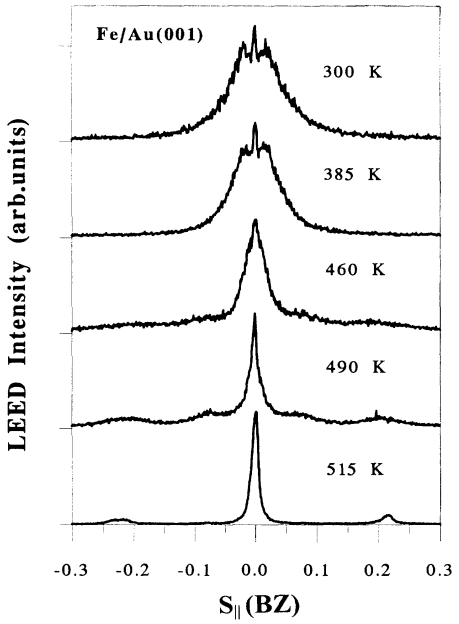


FIG. 4. The (00) beam angular profiles measured near the out-of-phase condition, 25.1 eV, and ~0.5 ML Fe coverage for various annealing temperatures.

dius and width only occur above ~400 K. This implies that significant surface diffusion occurs above ~400 K. As a result, the islands coalesce through surface diffusion, increasing the size and spacing with temperature. When the size and spacing of Au islands reaches at least twice the reconstruction unit mesh, ~2×(80 Å×14 Å) of clean Au(001) surface, the $\frac{1}{5}$ beams reappear.

We observed that the mechanism of atomic place exchange dominates the initial stage of growth, especially up to 1 ML coverage. There is evidence of nearly complete atomic place exchange up to ~3 ML under a similar growth condition. However, the process of atomic place exchange will be gradually suppressed in further growth especially when the Fe layer gets thick. For ~15 ML Fe/Au(001) films the surface is free of Au. A possible thickness dependence of the atomic place exchange was mentioned in the first-principles calculations [8]. The promotion of a floating Au layer on ~20 ML Fe/Au(001) films was reported in an Auger electron spectroscopy study [4], where the substrate temperature was held at ~420 to ~520 K during growth. This is similar to a sandwich formation in Rh/Ag(001) by high temperature annealing [5].

In summary, we have found that the submonolayer Fe films make atomic place exchanges with Au surface during room temperature growth. At ~0.5 ML coverage, the place exchanged Au adatoms and Fe atoms form 2D Au islands and Fe subsurface structures with a roughly equal island size and spacing. The sandwiched interface of submonolayer Fe/Au(00) films is structurally stable below ~380 K. Our result is consistent with recent first-principles calculations for a metal on metal system. This growth mode may be quite common in the heteroepitaxial ultrathin film growth.

We are grateful for the use of HRLEED from Leybold Vacuum Products. This work is supported by the ONR under Grant No. N00014-91-J-1099.

[1] P. J. Feibelman, Phys. Rev. Lett. **65**, 729 (1990); L. Hansen *et al.*, Phys. Rev. B **44**, 6523 (1991); T. J. Raeker, D. E. Sanders, and A. E. DePristo, J. Vac. Sci. Technol. A **8**, 3531 (1990); W. D. Luedtke and U. Landman, Phys. Rev. B **44**, 5970 (1991).

[2] S. C. Wang and G. Ehrlich, Phys. Rev. Lett. **67**, 2509 (1991); G. L. Kellogg and A. F. Voter, Phys. Rev. Lett. **67**, 622 (1991); G. L. Kellogg and P. J. Feibelman, Phys. Rev. Lett. **64**, 3143 (1990); C. Chen and T. T. Tsong, Phys. Rev. Lett. **64**, 3147 (1990).

[3] W. F. Egelhoff, Jr., Mater. Res. Soc. Symp. Proc. **229**, 27 (1991).

[4] S. D. Bader and E. R. Moog, J. Appl. Phys. **61**, 3729 (1987); S. D. Bader, J. Magn. Magn. Mater. **100**, 440 (1991).

[5] P. J. Schmitz *et al.*, Phys. Rev. B **40**, 11477 (1989); Vacuum **41**, 1411 (1990).

[6] S. Ino (to be published).

[7] S. Rousset *et al.*, Phys. Rev. Lett. **69**, 3200 (1992).

[8] C. T. Chan, K. P. Bohnen, and K. M. Ho, Phys. Rev. Lett. **69**, 1672 (1992).

[9] See, e.g., E. Bauer, Appl. Surf. Sci. **11/12**, 479 (1982).

[10] U. Scheithauer, G. Meyer, and M. Henzler, Surf. Sci. **178**, 441 (1986).

[11] See, e.g., M. G. Lagally, D. E. Savage, and M. C. Tringides, in *Reflection High-Energy Electron Diffraction and Reflection Electron Imaging of Surfaces*, edited by P. K. Larsen and P. J. Dobson (Plenum, New York, 1988), p. 139.

[12] Y.-F. Liew *et al.*, Surf. Sci. **273**, L461 (1992).

[13] P. Hahn, J. Clabes, and M. Henzler, J. Appl. Phys. **51**, 2079 (1980); H.-J. Ernst, F. Fabre, and J. Lapujoulade, Surf. Sci. **275**, L682 (1992), and references therein; J.-K. Zuo and J. F. Wendelken, Phys. Rev. Lett. **70**, 1662 (1993); B. Heinrich *et al.*, J. Appl. Phys. **70**, 5769 (1991); M. Henzler, H. Busch, and G. Friese, in *Kinetics of Ordering and Growth at Surfaces*, edited by M. G. Lagally (Plenum, New York, 1988), p. 101.

[14] J. M. Pimbley and T.-M. Lu, J. Appl. Phys. **57**, 1121 (1985); C. S. Lent and P. I. Cohen, Surf. Sci. **139**, 121 (1984).

[15] J. Wollschläger, J. Falta, and M. Henzler, Appl. Phys. A **50**, 57 (1990).

[16] J. Wollschläger and M. Henzler, Phys. Rev. B **39**, 6052 (1989); J. Falta, M. Horn, and M. Henzler, Appl. Surf. Sci. **41/42**, 230 (1989).

[17] Y.-L. He and G.-C. Wang, Mater. Res. Soc. Symp. Proc. **237**, 429 (1992).